Sodium interaction with ordered structures in mammalian red blood cells detected by Na-23 double quantum NMR

Hadassah Shinar, Tatyana Knubovets, Uzi Eliav, and Gil Navon
School of Chemistry, Tel Aviv University, Ramat Aviv 69978, Tel Aviv, Israel

ABSTRACT Na-23 double and triple quantum filtered NMR spectra of intact dog and human red blood cells were measured with the pulse sequence $90°-\tau/2-180°-\tau/2-\theta°-t_1-\theta°-t_2(\mathrm{Acq})$. For $\theta = 90°$ the triple quantum filtered spectra exhibited the typical multiple quantum filtered lineshape, characteristic of isotropic media, while the double quantum filtered ones presented a superposition of two signals, whose proportion depended on the creation time τ. This effect is due to the formation of both second and third rank tensors. The formation of the second rank tensor, T_{21} results from non-zero residual quadrupolar interaction and is related to the anisotropic motion of sodium ions. Measurements of the double quantum filtered spectra with $\theta = 54.7°$ enabled the detection of the contribution of T_{21} exclusively. No residual quadrupolar interaction was detected for sodium in the cytoplasm, while unsealed ghosts displayed the double quantum filtered spectral pattern, similar to that of intact cells. The anisotropy of motion of the sodium at the plasma membrane of mammalian erythrocytes depended on the integrity of the cytoskeleton network. Theoretical analysis of the double quantum filtered spectra gave a value of residual quadrupolar splitting of ~20 Hz for intact unsealed ghosts. The data presented prove that double quantum filtering is a sensitive technique for detection of motional anisotropies in biological systems.

INTRODUCTION

Recently we reported that Na-23 double quantum filtered (DQF) NMR spectra of bovine nasal cartilage displayed a superposition of two components, whose ratio varied with the creation time τ (1). We demonstrated that the effect is due to the formation of the second rank tensor resulting from the residual quadrupolar interaction of anisotropically moving sodium ions. The data indicate that order exists in this connective tissue. However, the question arises to what extent is the phenomenon specific for cartilage or occurs in other biological systems.

Mammalian red blood cells (RBC) have become the prototypal system for investigation of the plasma membrane structure and function. These cells are simply "bags" of hemoglobin rich cytosol and do not contain nuclei and intracellular organelles. The specific feature of RBC plasma membrane is the presence of well defined cytoskeleton (a dense protein shell which underlines the phospholipid bilayer). The major proteins of the cytoskeleton are spectrin and actin, which together comprise ~30% of the total protein content of the RBC membrane. The cytoskeleton plays a crucial role in the maintenance of the shape and deformability of the erythrocyte (2).

Here we report the detection of anisotropic motion of sodium in mammalian RBCs and their ghosts. Evidence is provided that the effect is determined by the integrity of the cytoskeleton.

EXPERIMENTAL

Dog venous blood was collected with heparin, kept at 4°C, and analyzed within 48 h. Dog RBCs have a high sodium concentration and were studied without further treatment.

Human venous blood was collected with EDTA (35 ml blood with 1 ml of 0.2 M EDTA) and kept at 4°C not more than 24 h. RBC were loaded with Na^+ by using nystatin as described previously (3). Erythrocytes were separated from plasma by centrifugation and washed three times with a solution containing 125 mM NaCl, 25 mM KCl, 5 mM Hepes, 10 mM glucose, pH 7.4. The cells were incubated for 30 min at 4°C in a solution containing 125 mM NaCl, 25 mM KCl, 0.6 mM NaH_2PO_4, 0.9 mM Na_2HPO_4, 27 mM sucrose, 10 mM glucose, 50 μg/ml nystatin, pH 6.7. The RBCs were washed four times with a 10-fold excess of the same solution devoid of nystatin, and then three times with a 10-fold excess of phosphate buffer saline. The resulting concentration of intracellular sodium was in the range 80–90 mM (3). RBCs were washed in solution containing 20 mM Hepes, 95 mM KCl, 12.5 mM $Na_5P_3O_{10}$, 5 mM $DyCl_3$, pH 7.4 immediately prior to NMR measurements. The final content of shift reagent (SR) $Dy(P_3O_{10})_2^{7-}$ was 5 mM and enabled a good separation of intra- and extracellular sodium signals (4).

Ghosts were prepared from human RBCs by means of hypoosmotic hemolysis at 4°C according to the original procedure of Dodge (5) modified by Fairbanks (6). Cells were separated from plasma by centrifugation and washed three times with solution containing 150 mM NaCl, 5 mM sodium phosphate buffer, pH 8.0. Erythrocytes were hemolyzed in a 40-fold excess of solution containing 5 mM sodium phosphate buffer, pH 8.0. Ghosts were sedimented by centrifugation and washed twice with the same solution. Finally the ghosts were washed once with solution containing 10 mM NaCl, pH 6.0. In order to increase the concentration of Na^+ aliquots of 1.5 M NaCl were added to the pellet of ghosts. The supernatant after the RBC hemolysis, which in fact presented a diluted erythrocyte cytosol, was concentrated to the final concentration of 5 mM hemoglobin by means of vacuum dialysis.

Ghosts were depleted of cytoskeleton according to traditional procedure, suggested by Fairbanks et al (6). A pellet of fresh ghosts was diluted tenfold with warm solution, containing 0.1 mM EDTA, 0.25 mM sodium phosphate buffer, pH 8.0 and incubated at 37°C for 30 min. Inside-out vesicles, resulting from this treatment of ghosts were sedimented at 4°C by centrifugation at 30,000 g for 120 min, and resuspended in solution containing 40 mM Hepes, 80 mM KCl, 50 mM NaCl, pH 7.4. The supernatant was analyzed for protein content. Selective proteolysis of band 3 was achieved by aging of ghosts at 4°C due to the activity of endogenous proteases.

The shape of the ghosts was analyzed by phase contrast microscopy. Inside-out-vesicles were studied by negative staining electron microscopy. Samples of ghosts and inside-out-vesicles were characterized by SDS-polyacrylamide gel electrophoresis (10% PAGE) according to the traditional procedure suggested by Laemmli (7). Protein content of the samples was assessed by the standard Bradford technique (8). The calibration was performed on albumin solution.

0006-3495/93/04/1273/07 $2.00

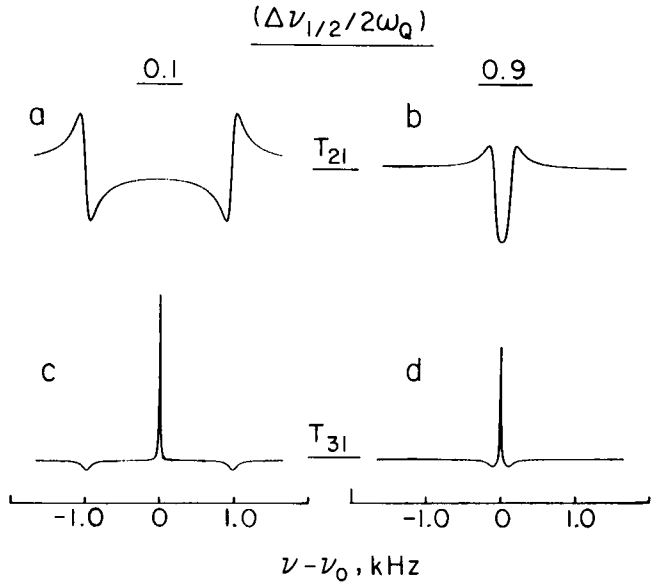

FIGURE 1 The contributions of the second rank tensor T_{21} (a, b) and the third rank tensor T_{31} (c, d) to the DQF spectra of $I = 3/2$ nuclei as a function of the ratio between the linewidth of the satellite transitions $\Delta\nu_{1/2}$ and the residual quadrupolar interaction ω_Q: $\Delta\nu_{1/2}/2\omega_Q$. The simulation is performed in the ideal case where all the binding sites are represented with a single value of ω_Q.

Na-23 NMR spectra were recorded at room temperature on AM-360-WB and AM-400-WB Bruker NMR spectrometers operating at 95.3 and 105.8 MHz for sodium-23, respectively. For detection of the multiple quantum coherencies the carrier frequency was adjusted on the measured signal. The double quantum filtered (DQF) or the triple quantum filtered (TQF) spectra were selected by a suitable phase cycling (9).

THEORETICAL BACKGROUND

DQF and TQF spectra were measured using the following pulse sequence (10, 11):

$$90°-\tau/2-180°-\tau/2-\theta°-t_1-\theta°-t_2(\text{Acq}), \qquad (1)$$

with $\theta = 90°$ and 54.7° for DQF and $\theta = 90°$ for TQF.

The first 90° pulse transfers the T_{10} tensor (z magnetization) into the single quantum coherences T_{11} and T_{1-1}. During the creation time τ quadrupolar relaxation in isotropic media causes evolution of T_{11} into T_{31} exclusively but in anisotropic media where average of the quadrupolar interaction ω_Q is nonvanishing, the second rank tensor T_{21} is formed as well. The time conjugate, T_{1-1}, undergoes similar time evolution. The 180° pulse serves to refocus chemical shifts and magnetic field inhomogeneity. The third pulse with $\theta = 90°$ transfers T_{31} into T_{32} and T_{33} and T_{21} into T_{22}, i.e., double and triple quantum coherences are formed and evolve during t_1. The last pulse transfers T_{32} and T_{33} into T_{31} and T_{22} into T_{21}, which evolve into the observable T_{11} during t_2. Phase cycling allows the selection of either DQ or TQ coherences. While the TQF experiment selects the contribution of the third rank tensor only, the DQF in anisotropic medium selects the contributions of both third rank (T_{32}) and second rank (T_{22}) tensors. However by a judicial choice of $\theta = 54.7°$ the formation of T_{32} is eliminated and only the contribution of T_{22} appears in the spectrum (1, 11, 12).

In isotropic medium the formation of T_{31} results in detection of two absorptive lines in antiphase (10, 11).

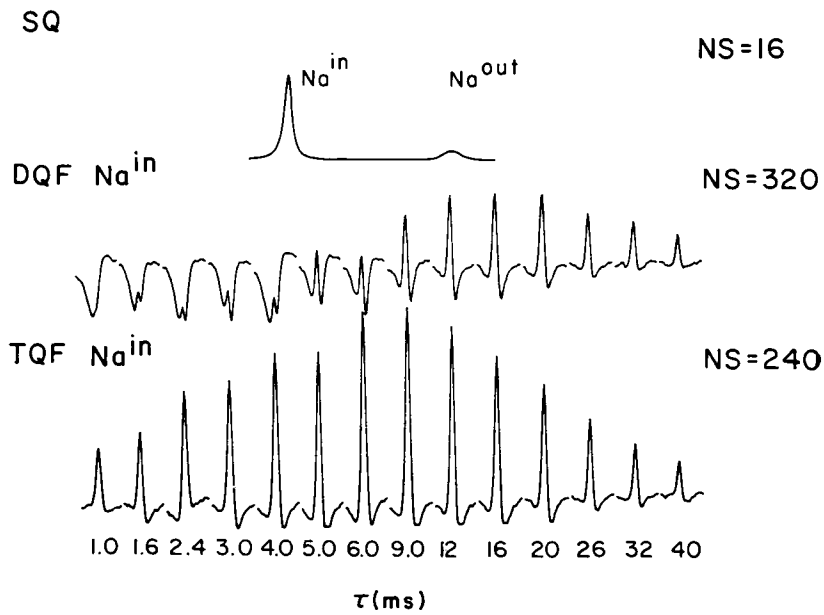

FIGURE 2 SQ, DQF, and TQF Na-23 NMR spectra of intact dog red blood cells suspended in the presence of 5 mM of shift reagent $(Dy(TPP)_2)^{7-}$ (see Experimental Section). DQF and TQF spectra are shown only for the intracellular Na-23 signal. DQF and TQF spectra were measured with pulse sequence (1) with $\theta = 90°$ and various creation times τ.

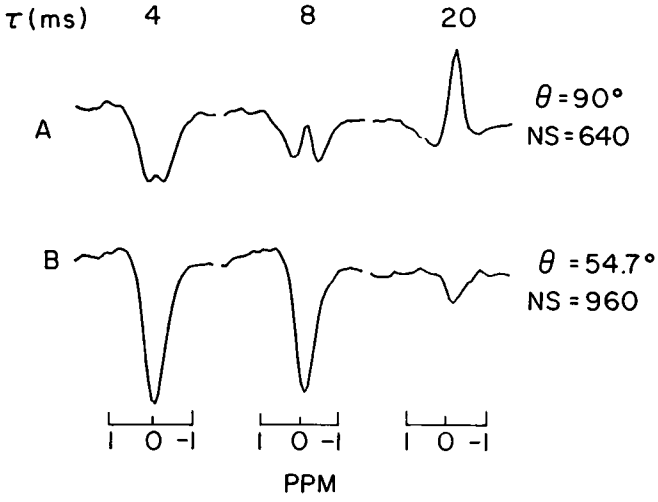

FIGURE 3 Intracellular signal in DQF spectra of Na^+-loaded human red blood cells suspended in the presence of 5 mM of $Dy(TPP)_2^{7-}$. The cells were loaded with sodium by means of treatment with nystatin (see Experimental Section). Na-23 DQF NMR spectra were measured with the pulse sequence (1) with $\theta = 90°$ (*A*) and $\theta = 54.7°$ (*B*) at various creation times τ.

In anisotropic medium the spectrum is more complicated and presents a combination of three absorptive lines, the central band and two satellites in antiphase to it. The formation of T_{21} results in detection of a broad component presenting in fact pairs of overlapping dispersive lines of the satellites in antiphase. The splitting is equal to the residual average of quadrupolar interaction, $2\omega_Q$. The simulated contributions of T_{31} and T_{21} tensors for the ideal case of a single value of ω_Q provide a good visualization of the lineshape dependence on the ratio between ω_Q and the linewidth (Fig. 1). When ω_Q is much larger than the linewidth, like in liquid crystals, the contributions of the second rank (T_{21}) and the third rank (T_{31}) tensors are presented in Fig. 1 *a* and Fig. 1 *c*, respectively. In such a case the presence of splitting is also evident from the single quantum (SQ) spectrum. When ω_Q is of the order of magnitude of the linewidth, the anisotropy cannot be detected by SQ spectra. The contributions of T_{21} and T_{31} to the DQF spectra are given in Fig. 1, *b* and *d*, respectively.

Theory predicts that contribution of the T_{21} is increased 1.5-fold for $\theta = 90°$ as compared to $\theta = 54.7°$ (13). Thus, it is possible to exclude the contribution of T_{21} and select that of T_{31} by taking the difference between the DQF spectra measured with $\theta = 90°$ and that measured with $\theta = 54.7°$ with 50% more accumulations.

RESULTS

In Fig. 2 Na-23 SQ, DQF and TQF spectra of intact dog RBCs, suspended in the medium containing SR, are given. The TQF spectra of the intracellular Na-23 signal exhibit the typical multiple quantum filtered lineshape, characteristic of isotropic medium. The lineshape remains almost invariable for the whole range of creation times, and only the amplitude is modulated. In contrast, the DQF spectra present a superposition of two components, whose proportion depends on τ. The broad component is dominant at short creation times, but then disappears, while the narrow one still evolves at longer τ values. This pattern is analogous to that we reported recently for bovine nasal cartilage (1) and is in full agreement with the theoretical considerations presented above: the narrow component results from the formation of T_{31}, while the broad one in DQF, from that of T_{21}. Similar data were obtained for fresh and Na^+-loaded human RBCs (Fig. 3). Na-23 DQF spectra measured with the pulse sequence (1) with $\theta = 54.7°$ detect only the broad component, which is a result of the contribution from T_{21} exclusively, again in agreement with the theoretical considerations.

To examine the contribution of each of the RBC components to the anisotropic motion of the sodium ions a Na-23 DQF study of separated cytosol and plasma membranes from human erythrocytes was performed. In case of the cytosol the Na-23 DQF spectra did not display the pattern typical for anisotropic motion and for $\theta = 54.7°$ the signal was negligible. For intact unsealed ghosts we found that Na-23 DQF signal is similar to that observed for intact RBCs (Fig. 4). Measurement of DQF spectra with pulse sequence (1) with $\theta = 54.7°$ and their subsequent subtraction from those registered with $\theta = 90°$ resulted in deduction of the contributions from the T_{21} and the T_{31} separately. These data prove that anisotropic motion of sodium ions in RBC is due to their interaction with plasma membrane.

Further experiments were aimed at the elucidation of sources of anisotropy in plasma membrane of human RBCs. Cytoskeleton depleted inside-out vesicles with the diameter ~ 1 μm are produced as a result of spectrin and actin extraction from the ghosts. The selective depletion of spectrin and actin is proved by gel electrophoresis (PAGE with SDS) (Fig. 5). In intact ghosts one can clearly see the α- and β- chains of spectrin as well as actin and band 3. The amount of spectrin and actin in the preparation of depleted ghosts is drastically reduced, while band 3 is practically unchanged. The extracted cytoskeleton proteins are readily registered in the supernatant. These sealed inside-out vesicles may serve as a model for the inner side of the plasma membrane devoid of the cytoskeleton. Na-23 DQF spectra of the vesicles exhibit the multiple quantum filtered lineshape typical for isotropic motion, i.e., a drastic decrease in the contribution of T_{21} as compared to T_{31} occurs. Moreover, cytoskeleton depletion of ghosts was accompanied by a significant diminution of the intensity of Na-23 DQF signal relative to that of the SQ.

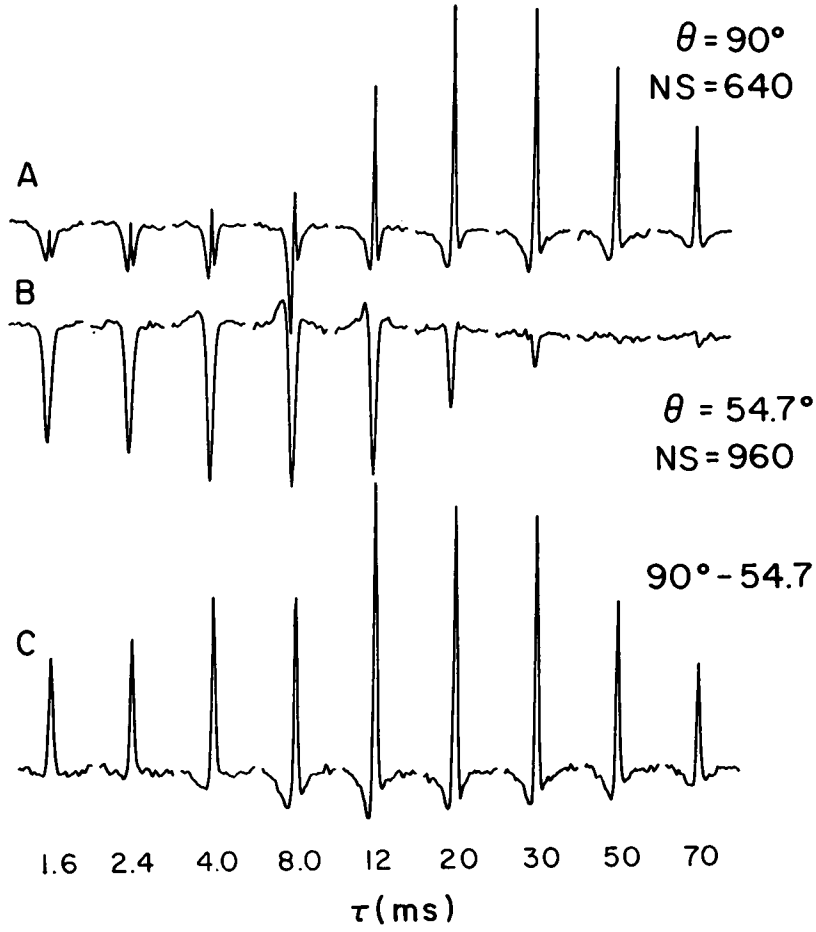

FIGURE 4 Na-23 DQF NMR spectra of suspension of intact unsealed ghosts (4 mg protein/ml) measured with the pulse sequence (1) with $\theta = 90°$ (A), $\theta = 54.7°$ (B), and their difference ($C = A - B$).

Another indication to the cytoskeleton involvement in the anisotropy of sodium motion at the membrane is obtained from the drastic dependence of the effect on the ionic strength of the suspending solution (Fig. 6). For ghosts in 10 mM NaCl the contribution of T_{21} to Na-23 DQF spectra with $\theta = 90°$ was negligible, and for $\theta = 54.7°$ practically no signal was detected. At the same time the DQF signal was surprisingly intensive relative to that of the SQ. An increase in the NaCl concentration in the suspending medium to 50 mM resulted in the detection of a typical anisotropic pattern. The amplitude ratio of the T_{31} to that of SQ was decreased as compared to 10 mM NaCl, while the relative proportion of T_{21} was drastically increased. The increase in the NaCl concentration from 10 to 50 mM is accompanied by changes in the shape of the ghosts from cup-shaped to a shape close to a regular discocyte. Further increase in the ionic strength did not cause any significant changes either in the pattern of the Na-23 DQF spectra, or in the shape of the ghosts. The dependence of the anisotropy on ionic strength of the suspending solution is in agreement with conformational changes of the cytoskeleton in the same range of NaCl concentrations already found by traditional biochemical techniques (14).

Selective proteolysis of band 3 was achieved by aging of the ghosts at 4°C. Gel electrophoresis unambiguously proves that complete proteolysis of band 3 was achieved (Fig. 5). This treatment of ghosts was not accompanied by any significant changes in their shape. Since the cytoskeleton is attached to the phospholipid bilayer via two anchoring sites: to band 3 (via ankyrin), and to glycophorin C (via band 4.1) (2), the proteolysis of band 3 may cause a detachment of the whole network from the membrane. Fig. 7 demonstrates that band 3 proteolysis of the ghosts is accompanied by a diminution of Na-23 DQF signal intensity and the contribution of T_{21} is decreased to the larger extent.

In order to check the validity of our theoretical interpretation we have chosen to analyze the Na-23 DQF spectra of intact unsealed ghosts of human RBCs. The analysis of intact erythrocytes was more complicated due to the contribution of the interaction of sodium with the intracellular proteins to the spectra and the use of SR. The experimental data were fitted to the following

TABLE 1 **Spectral densities and residual quadrupolar splitting that were obtained by a fit of the experimental data to the theoretical model described in the text**

J_0 (Hz)*	J_1 (Hz)*	J_2 (Hz)*	ω_Q^{Loc}	$\Delta\omega_Q^{Loc}$
18.5	3.5	1.8	22.3	10.5

* Spectral densities.

model (1, 13 model c): (*a*) DQF spectra are a result of the time evolution of the second (T_{21}) and the third (T_{31}) rank tensors; (*b*) both tensors are formed as a result of the evolution of T_{11} under the nonvanishing quadrupolar interaction and multiexponential relaxation; (*c*) the value of ω_Q in the laboratory frame of reference (with z direction along the magnetic field) is given in terms of its value, ω_Q^{Loc}, in a local director frame of reference by the following transformation:

$$\omega_Q^{Lab} = \omega_Q^{Loc}(3\cos^2\theta_{LD} - 1)/2, \qquad (2)$$

where θ_{LD} is the angle between the local director and the magnetic field; (*d*) a symmetrical Gaussian distribution of ω_Q^{Loc} with a width $\Delta\omega_Q^{Loc}$ (15) is assumed in order to take into account the heterogeneity of the system. The nonequivalence of the binding sites is unequivocally deduced from the variations of the linewidth of the T_{21} contributions to the observed spectra as a function of τ. These variations imply that the chemical exchange between sites with different ω_Q^{Loc} and θ_{LD} is slow; (*e*) a fast

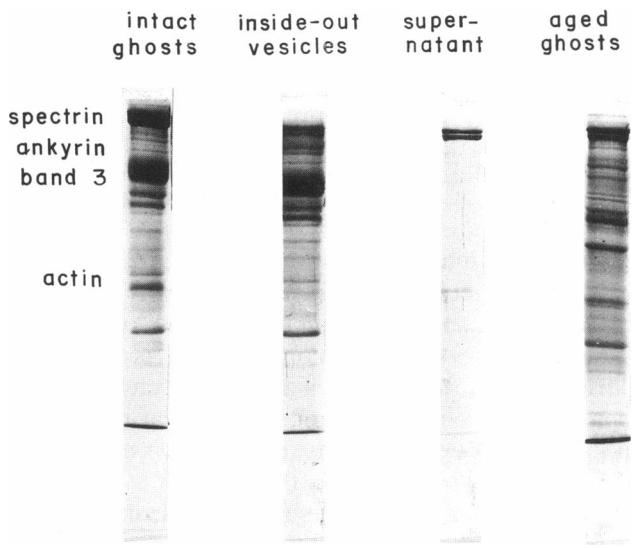

FIGURE 5 SDS-PAGE (10%) of (*a*) fresh intact ghosts (5 μl of a fixed sample, containing 1 mg protein/ml), (*b*) inside-out vesicles (5 μl of a fixed sample, containing 1.3 mg protein/ml), (*c*) supernatant, obtained after the preparation of inside-out vesicles (30 μl of a fixed sample, containing 0.05 mg protein/ml), and (*d*) aged ghosts, (10 days old), (5 μl of a fixed sample, containing 1 mg protein/ml), the same preparation as *a*.

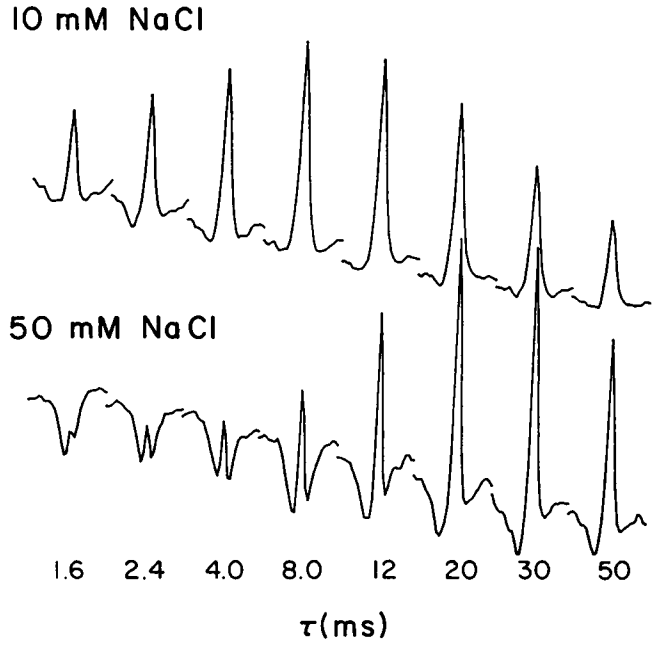

FIGURE 6 Na-23 DQF NMR spectra of suspension of intact unsealed ghosts (4 mg protein/ml) measured with the pulse sequence (1) with $\theta = 90°$. The suspending medium contained 10 mM NaCl (*top*) and 50 mM NaCl (*bottom*).

chemical exchange between sodium in the bulk solution in the vicinity of the binding sites and the sites themselves is assumed. The latter assumption is based on the similarity of the longitudinal relaxation times of sodium ions in the suspension of ghosts and in saline. Fig. 8 shows a fitting of DQF spectra of intact unsealed ghosts measured with the pulse sequence (1). The values obtained for the spectral densities and the residual quadrupolar interaction are given in Table 1.

DISCUSSION

We have recently shown for Na-23 in cartilage that the formation of the second rank tensor is a sensitive marker for the presence of ordered structures in biological tissue (1). In the present work we show that this method can serve to detect anisotropic motion of sodium in mammalian erythrocytes. The effect of anisotropy persists in RBC ghosts but is completely undetectable in the separated cytoplasm. We have thus deduced that the anisotropic motion originates from the interaction of sodium with the plasma membrane. More specifically we have evidence that it is related to the integrity of the cytoskeleton. This point is however quite hard to prove as any changes in the cytoskeleton network inevitably affect morphology of erythrocytes and their ghosts.

The dramatic decrease in the T_{21} contribution to Na-23 DQF NMR spectra of cytoskeleton depleted membranes suggests that the presence of the network is rele-

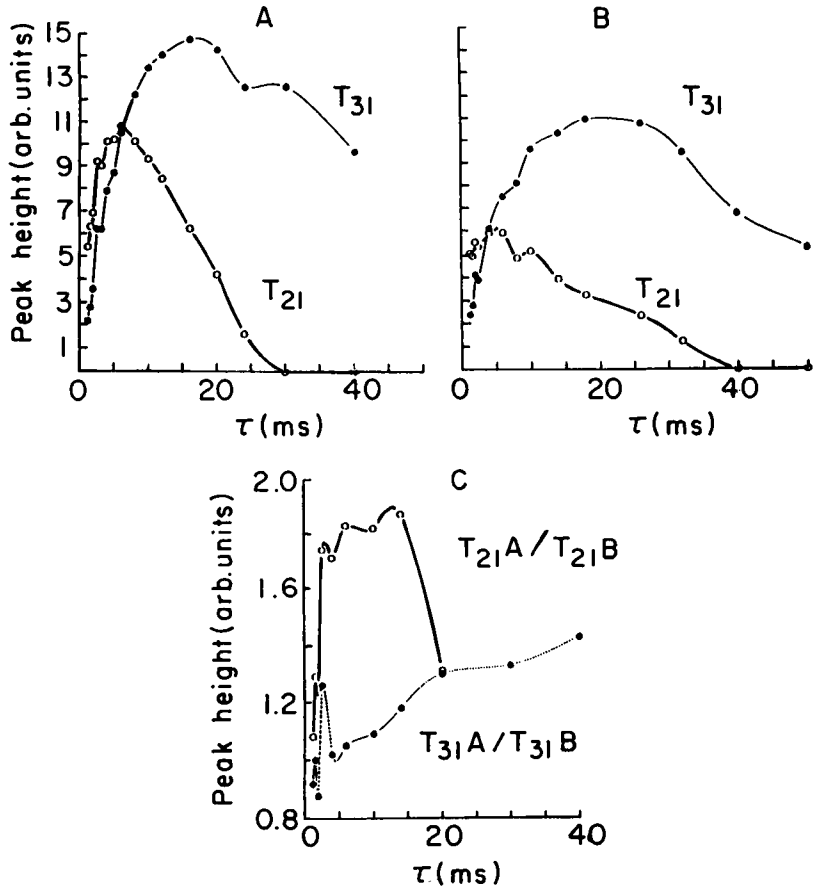

FIGURE 7 The contribution of T_{31} and T_{21} to the Na-23 DQF NMR spectrum as a function of creation time, τ: (*A*) intact and (*B*) band 3 proteolized ghosts. (*C*) Relative decrease in the both components T_{21} and T_{31} in the result of aging of the ghosts.

vant for the anisotropy of sodium motion. However, depletion of spectrin and actin from intact ghosts results in disintegration of the membrane and the formation of inside-out vesicles with the diameter ≤ 1 μm. The faster Brownian motion of these species as compared to the 7 μm diameter ghosts may by itself lead to an averaging of the residual anisotropy to zero. Therefore, in this case the disappearance of anisotropy cannot be unequivocally associated with the loss of the cytoskeleton.

Two other experiments were designed to induce only minor changes in the cytoskeleton network. The first of them is based on a dependence of the cytoskeleton conformation on the ionic strength of the suspending solution. Our results indicate that when intact unsealed ghosts are suspended in a medium with low ionic strength, and obtain a cup-shape form, no anisotropy is detected. On the other hand in case of ghosts suspended in 50 mM NaCl, when their shape is already close to a discocyte, the anisotropic pattern is clear. This drastic change in the T_{21} contribution to DQF spectra is not accompanied by any changes in the total size of the ghosts, which is around 7 μm. Further increase in ionic strength did not produce any changes in the Na-23 DQF NMR spectra and the ghost shape also did not change significantly. It is well known that drastic conformational changes take place in the cytoskeleton of ghosts suspended in 10 mM NaCl. At this salt level the major dissociation of spectrin tetramers to dimers inside the ghost membrane was observed (14). The dissociation is accompanied by a decrease in the percentage of the α-helical regions in the spectrin molecules (16), which might be the major reason for loosening of the whole cytoskeleton network and the loss of anisotropy.

Another experiment, which produced only minor changes in the cytoskeleton conformation, is aging of the ghosts. Here we detected a significant decrease in T_{21}, representing the nonvanishing quadrupolar interaction. In this experiment the ghosts retained their original size with no noticeable change in their shape.

The model used in the present study assumes regions of free sodium exchanging with sodium bound in ordered sites. The latter gave rise to the formation of the second rank tensor. The directors in these regions are randomly oriented, but the exchange between them is not fast enough to annihilate the effect. One set of parameters was sufficient to reproduce spectra originating from both T_{21} and T_{31} for the whole range of creation times. These values are weighted averages of the free and bound

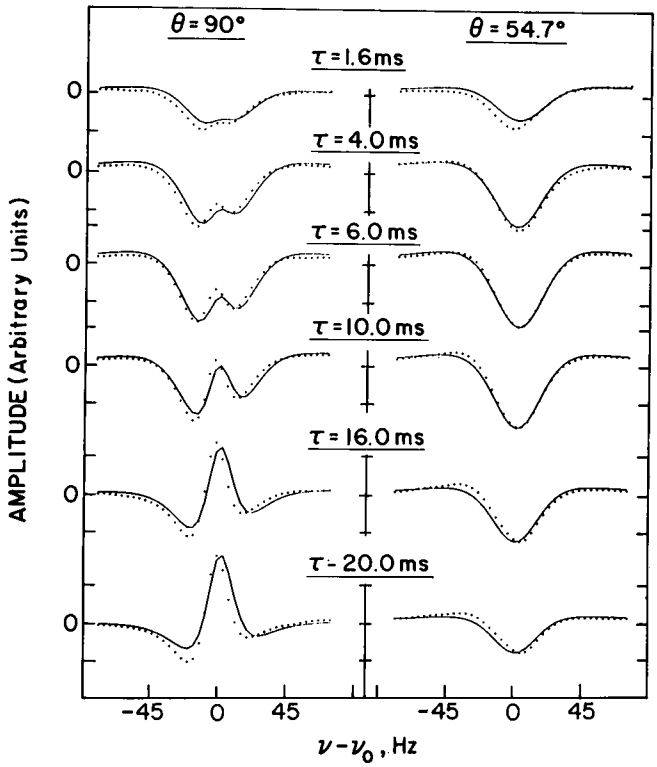

FIGURE 8 Simulation of Na-23 DQF NMR spectra of intact unsealed ghosts suspended in 75 mM NaCl. DQF spectra were measured with pulse sequence (1) with $\theta = 90°$ and $\theta = 54.7°$ at various creation times τ. (· · ·) Experimental spectra; (——) simulated spectra.

sodium and are a function of the bound fraction. In a system of intact ghosts we obtain a value of ω_Q of ~20 Hz from our theoretical fit. If we assume the quadrupolar coupling constant χ of 1.5 MHz, the product of the fraction of bound sodium P_B and the order parameter $P_B \times S = 3 \times 10^{-5}$. This is an order of magnitude smaller than the value obtained for cartilage (13). Typical values for liquid crystals are of the order of 10^{-2}.

The method presented here for the detection of anisotropic movement is extremely sensitive and a residual quadrupolar interaction of the order of magnitude of the linewidth can be detected. Thus by DQF techniques both the dynamics of the bound sodium as well as the order of the system can be studied.

This work was supported by the Israeli Ministry of Science and Technology.

The authors are grateful to Professor A. Loewenstein and Professor H. Gilboa from the Faculty of Chemistry, the Technion, Israel Institute of Technology, Haifa, for kindly allowing the use of their NMR spectrometer. We are grateful to Mrs. J. Zipser for assistance with gel electrophoresis experiments, and to Dr. S. Levin for fruitful discussions and help with phase contrast microscopy of ghosts.

Received for publication and in final form 22 September 1992.

REFERENCES

1. Eliav, U., H. Shinar, and G. Navon. 1992. The formation of a second rank tensor in Na-23 double quantum filtered NMR as an indicator for order in a biological tissue. *J. Magn. Reson.* 98:223–229.
2. Darnell, J., H. Lodish, and D. Baltimore. 1990. Molecular Cell Biology. Scientific American Books, New York. 1105 pp.
3. Knubovets, T. L., A. V. Revazov, L. A. Sibeldina, and U. Eichhoff. 1989. ^{23}Na NMR measurement of the maximal rate of active sodium efflux from human red blood cells. *Magn. Reson. Med.* 9:261–272.
4. Gupta, R. K., and P. Gupta. 1982. Direct observation of resolved resonances from intra- and extracellular sodium-23 ions in NMR studies of intact cells and tissues using dysprosium (III) tripolyphosphate as paramagnetic shift reagent. *J. Magn. Reson.* 47:344–350.
5. Dodge, J. T., C. Mitchell, and D. J. Hanahan. 1963. The preparation and chemical characteristics of hemoglobin-free ghosts of human erythrocytes. *Arch. Biochem. Biophys.* 110:119–130.
6. Fairbanks, G., T. L. Steck, and D. F. H. Wallach. 1971. Electrophoretic analysis of the major polypeptides of the human erythrocyte membrane. *Biochemistry* 10:2606–2617.
7. Laemmli, U. K. 1970. Cleavage of structural proteins during the assembly of the head of bacteriophage T_4. *Nature (Lond.).* 227:680–685.
8. Bradford, M. 1976. A rapid and sensitive method for the quantitation of microgram quantities of protein using the principle of protein-dye binding. *Anal. Biochem.* 72:248–254.
9. Bodenhausen, G., H. Kogler, and R. R. Ernst. 1984. Selection of coherence-transfer pathways in NMR pulse experiments. *J. Magn. Reson.* 58:370–388.
10. Pekar, J., and J. S. Leigh. 1986. Detection of biexponential relaxation in sodium-23 facilitated by double-quantum filtering. *J. Magn. Reson.* 69:582–584.
11. Jaccard, G., S. Wimperis, and G. Bodenhausen. 1986. Multiple quantum NMR spectroscopy of S = 3/2 spins in isotropic phase: a new probe for multiexponential relaxation. *J. Chem. Phys.* 85:6282–6293.
12. Furo, I., and B. Halle. 1991. Methods for NMR studies of I > 1 nuclei in anisotropic systems with small quadrupole splitting. *Chem. Phys. Lett.* 182:547–550.
13. Eliav, U., and G. Navon. 1992. Analysis of double quantum filtered NMR spectra of ^{23}Na in biological tissues. *J. Magn. Reson.* In press.
14. Liu, Sh.-Ch., and J. Palek. 1980. Spectrin tetramer-dimer equilibrium and the stability of erythrocyte membrane skeletons. *Nature (Lond.)* 285:586–588.
15. Rooney, W. D., and C. S. Springer, Jr. 1991. A comprehensive approach to the analysis and interpretation of the resonances of spins 3/2 from living systems. *NMR Biomedicine.* 4:209–226.
16. Ralston, G. B., and J. C. Dunbar. 1979. Salt and temperature-dependent conformation changes in spectrin from human erythrocyte membranes. *Biochim. Biophys. Acta.* 579:20–30.